Brief report: Chronic murine schistosomiasis causes aberrant hemostasis

Joanna H. Greenman[a,b], Lucie Moss[a,b], Shinjini Chakraborty[a,b], Bradley J. Whitehead[c,d], Johan Palmfeldt[c], Peter Nejsum[c,d], James P. Hewitson[a,b]*, and Ian S. Hitchcock[a,b]*

[a]*Department of Biology, University of York, Heslington, York, United Kingdom;* [b]*York Biomedical Research Institute, University of York, Heslington, York, United Kingdom;* [c]*Department of Clinical Medicine, Aarhus University, Aarhus, Denmark;* [d]*Department of Infectious Diseases, Aarhus University Hospital, Aarhus, Denmark*

Schistosomiasis afflicts >250 million people worldwide, leading to an annual loss of >3 million disability-adjusted life years. *Schistosoma mansoni* causes intestinal schistosomiasis with parasite eggs either transversing intestinal tissue or lodging within the liver and other organs, causing intestinal hemorrhage and liver pathology. Large (~1 cm) adult worms survive for years within blood vessels, but we lack a clear understanding of their impact on hemostasis. We used a chronic mouse model of schistosomiasis to determine the impact on platelet numbers, phenotype and function. Hemostatic function was assessed by platelet phenotyping (flow cytometry and proteomics), whole blood aggregometry, and longitudinal coagulometry. Although platelets from schistosome-infected mice lack elevated surface P-selectin and activated αIIbβ3, unbiased proteomic analysis reveals infection-induced increases in MHC-I, IgM and IgG antibodies, and complement components. Whole blood from schistosome-infected mice spontaneously aggregates in the absence of exogenous agonists. Conversely, prothrombin and activated partial thromboplastin times are prolonged at the chronic stage of infection (10–12 weeks). A mouse model of *S. mansoni* infection shows wide-ranging changes in hemostatic function which may have clinically relevant implications for populations in endemic regions.

HIGHLIGHTS

- Schistosomiasis causes thrombocytopenia and spontaneous whole blood aggregation.
- Platelet proteomics reveals marked changes in protein expression without increased P-selectin or integrin activation.
- Longitudinal analysis shows prolonged coagulation (prothrombin time and activated partial thromboplastin time) during chronic infection.

Schistosomiasis is a chronic parasitic disease caused by platyhelminth parasites of the genus *Schistosoma* [1]. In 2019, the World Health Organization (WHO) estimated over 250 million people were infected and 800 million were at risk of infection with >90% disease occurring in sub-Saharan Africa [2]. Disease morbidity leads to an annual loss of 3.3 million disability-adjusted life years [3]. Infection occurs when free-living cercariae released from freshwater snails penetrate host skin, migrate through venous circulation, and eventually reach the liver. Here, adult worms develop and migrate into mesenteric (*S. mansoni* and *S. japonicum*) or bladder wall (*S. haematobium*) blood vessels. From 4 to 5 weeks postinfection, sexually mature female worms release hundreds of eggs each day. These either successfully exit the host via fecal or urinary routes to allow onward transmission, or alternatively lodge within tissues including the liver, bladder and lung. Eggs induce strong type 2 immune responses and granulomatous inflammation that transitions through acute (6–8 weeks) to chronic stages (10 weeks+), and adult worms can survive in blood vessels for many years, feeding on blood contents [1].

Several studies have assessed the impact of schistosome infection on hemostasis [4–7]. Human infection can lead to thrombocytopenia (platelet counts $<100 \times 10^9$/L), which occurs in >95% of those with hepatosplenic disease [5], alongside increased activated partial thromboplastin time (aPTT), D-dimer levels, and fibrin degradation products [4,6,7]. Together, this suggests impaired thrombus formation, consistent with infection-induced bleeding pathologies. Mouse models offer the advantage of allowing infective dose and duration to be controlled, and unlike controlled human schistosome infections [8], the impact of egg-induced disease pathology can be determined. A small number of animal studies have assessed the impact of acute schistosome infection on blood parameters after high dose infections (i.e., 7–8 weeks postinfection with 80–200 cercariae) [9–11]. However, such infections are soon fatal due to excessive egg-induced pathology, and so do not reflect the chronic nature of human schistosomiasis where pathology accumulates over many years [1]. As such, we lack a good understanding of the longitudinal impact of chronic

Address correspondence to James P. Hewitson and Ian S. Hitchcock, Department of Biology, University of York, Heslington, York YO10 5DD, United Kingdom; E-mails: james.hewitson@york.ac.uk, Ian.hitchcock@york.ac.uk

0301-472X/

https://doi.org/10.1016/j.exphem.2024.104689

Table 1 Flow cytometry and confocal microscopy antibodies.

TARGET	Clone	Fluorochromes	Supplier	Dilution
Flow cytometry				
CD41	MWReg30	FITC, PE, APC, A700	Biolegend	1:500
CD61	2C9.G2	PE	Biolegend	1:500
CD62L	MEL-14	PE	Biolegend	1:500
JON/A	JON/A	PE	Emfret	1:250
CD62P	RMP-1	PE-Cy7	Biolegend	1:250
MHC-I (H-2)	M1/42	FITC	Biolegend	1:250
Confocal microscopy				
TPO	EPR14948	Unconjugated (rabbit)	eBioscience	1:100
CD41	MWReg30	Biotin	Biolegend	1:200
α-Rabbit IgG	Chicken pAb	A647	Invitrogen	1:400
Streptavidin	n/a	A546	Biolegend	1:400

schistosomiasis on coagulation and hemostasis. To address this, we carried out platelet phenotyping, aggregometry and longitudinal coagulometry on mice infected with low (non-fatal) doses of *S. mansoni*.

METHODS

S. mansoni Infection

Ethical approvals for animal studies were obtained from University of York Animal Welfare and Ethical Review Body. All procedures were performed under the authority of UK Home Office Project Licenses PFB579996, PP5712003, and P49487014. Female C57BL/6 mice (7–12 weeks old at start of experiment) were housed in individually ventilated cages under specific pathogen-free conditions with food and water *ad libitum*. Mice were anesthetized (medetomidine, ketamine) and infected with 35–50 *S. mansoni* cercariae by percutaneous penetration of the shaved abdomen. In other experiments when indicated in the figure legend, mice were infected with 25, 50 or 100 cercariae to assess the impact of varying parasite dose. Schistosome-infected *Biomphalaria glabrata* snails were provided by the Barrett Centre for Helminth Control (Aberystwyth University, UK). Mice infected with 25–50 cercariae were culled at 12 weeks post-infection. Mice infected with 100 cercariae were culled at 7 weeks post-infection as they will not survive until later time points.

Platelet Quantification and Characterization Using Whole Blood

Blood was obtained from free-flowing tail or saphenous veins into Microvette CB 300 K2 EDTA capillary blood collection tubes (Sarstedt). Complete blood cell counts were performed with a SCIL Vet ABC Plus analyzer. Annexin V staining was carried out at room temperature (RT) with 5–10 μL of blood in 100 μL PBS stained with CD41-PE (0.2 μg MWReg30, Biolegend, 30 min), washed with phosphate-buffered saline (PBS) and Annexin V Binding Buffer (eBioscience), and then stained with 5 μL Annexin V–APC (eBioscience, 15 min). All centrifugation steps were carried out at 350 $\times$ *g* (5 min). Samples were washed and resuspended in Binding Buffer before immediate flow cytometry analysis (BD-LSRFortessa).

Platelet Isolation and Characterization

Cardiac puncture was performed on terminally anesthetized mice and blood mixed with acid citrate dextrose (ACD) buffer (1:9) and an equal volume of 2%$_{(v/v)}$ FCS/PBS Wash Buffer added. For flow cytometry, platelet rich plasma (PRP) was obtained by centrifugation at 60 $\times$ *g* (7 min, room temperature (RT), slow acceleration, no break). Platelets were pelleted by centrifugation at 240 $\times$ *g* (10 min, RT), resuspended in 500 μL Wash Buffer and counted (Beckman Coulter Z1D cell counter). Where indicated, platelets were activated with 150 μM Protease-Activated Receptor 4 (PAR4) agonist (AYPGKF-NH2, Fisher Scientific) for 10–30 min in Wash Buffer at RT, washed, and stained using antibodies in Table 1. MHC-I expression on platelets and leukocytes was analyzed using whole blood. For proteomic analysis, cardiac blood collected in ACD as above underwent 3 sequential 60 $\times$ *g* centrifugations to deplete red blood cells, followed by 3 PBS + 1 U/mL apyrase and 1 μM prostaglandin E1 washes (Sigma) at 240 $\times$ *g* to deplete plasma proteins and pellet platelets. Recovered platelets were resuspended in 200 μL lysis buffer (4% SDS in 0.1M Tris-HCl pH 7.6) and stored at −80°C.

Platelet Proteomics

In-gel trypsin digest and liquid chromatography tandem mass spectrometry (LC-MS/MS) analysis of platelet lysates was performed as previously described [12]. Peptides were analyzed using a nano-LC (Easy-nLC 1200)-tandem-MS (Q-Exactive HF-X Hybrid Quadrupole Orbitrap, Thermo Fisher Scientific). Protein hits were identified with MaxQuant (v1.5.3.30) and UniProt mouse database [13]. Matching between runs was performed and iBAQ intensities were used to determine differential expression using Perseus v2.0.11 [14]. Proteins with valid values in >70% of samples in at least one group were used for analysis. Differentially expressed proteins ($p \leq 0.05$, fold change $\geq$2 or $\leq$-2) were filtered with a permutation-based false discovery

rate. Bioinformatic analysis was performed using Enrichr [15]. Full proteomics data will be deposited at PRIDE (https://www.ebi.ac.uk/pride/).

Aggregometry and Coagulometry

For whole blood aggregometry, blood was collected by cardiac puncture into anticoagulant citrate dextrose (ACD) and diluted 1:2:2 (blood:0.9%$_{(w/v)}$ saline:Ringer's buffer with 2 mM $CaCl_2$). Impendence was measured for 10 min at 37°C with constant stirring using a Chronolog-700 aggregometer. For longitudinal coagulometry, whole blood (40 μL) was transferred directly from the saphenous vein puncture site onto Coag Dx* PT or aPTT cartridges and analyzed using a Coag Dx* analyzer (IDEXX UK).

Confocal Microscopy

Cryosections (8–10 μm) were cut from liver samples frozen in OCT (CellPath) using a Leica CM 3050S cryostat and transferred to SuperFrost+ slides (VWR). Sections were fixed in ice-cold acetone (5 min) and subsequent steps carried out at RT. Sections were washed in 0.5% BSA/PBS$_{(w/v)}$ wash buffer, blocked 5% rat serum in wash buffer (30 min), avidin-biotin blocked (Lab Vision Avidin biotin Blocking Solution, ThermoFisher), and washed 3 times in wash buffer. Sections were incubated with antibodies against CD41 and TPO for 1 hour, washed twice in wash buffer, incubated with fluorochrome-conjugated antibodies/streptavidin for 45 min (Table 1), washed, stained for 5 min with 1 μg/mL 4′,6-diamidino-2-phenylindole (DAPI, Sigma), and mounted with ProLong Gold (ThermoFisher). Sections were imaged using a Zeiss LSM780 confocal microscope and analyzed with Zeiss Zen and Fiji ImageJ software.

RESULTS AND DISCUSSION

Thrombocytopenia can be caused by a diverse range of immune challenges [16–18] including *S. mansoni* infection [4–7]. Here, we used a mouse model of chronic schistosomiasis to assess the kinetics, phenotypic impact and functional consequences of infection on platelets. Schistosome infection caused thrombocytopenia at 4 weeks post-infection (i.e., around the start of egg production) which was sustained until the chronic phase (weeks 10–12) when experiments were terminated (Figure 1A). Mean platelet volume (MPV) increased, particularly after 8 weeks which coincides with acute inflammation caused by parasite eggs (Figure 1B). This likely reflects bone marrow stress and a predominance of larger immature platelets [19]. We next assessed whether changes in platelet numbers and size were associated with altered function. The surface tegument of adult worms contains multiple phosphatases suggested to interfere with platelet aggregation [20–22] but their impact in live infection is less clear. Surprisingly, we found platelets in whole blood from schistosome-infected animals spontaneously aggregate in the absence of exogenous agonist and, in some cases, clotted before aggregometry analysis even after a successful blood draw (<2 min after sample collection) (Figure 1C, D). We next tested whether spontaneous platelet aggregation reflected an activated phenotype by measuring active αIIbβ3 integrin (using JON/A mAb) and surface P-selectin [23,24], but this revealed no difference between naive and infected mice, and both groups of platelets responded similarly to PAR4 agonist (Figure 1E, F). Platelets from infected mice did have elevated surface phosphatidylserine (PS) which can promote phagocytic clearance and drive the intrinsic and common pathways of the coagulation cascade [25–27] (Figure 1G). To gain a greater understanding of infection-induced changes, we conducted an unbiased proteomic comparison of platelets from naive and infected mice. We identified 1,005 proteins, of which 94 were significantly differentially expressed (DE) between naive and infected mice (Figure 1H and Supplementary Table E1). The vast majority of DE proteins (89/94 = 95%) were upregulated in infection (Figure 1I) including haptoglobin, MHC class I and β2-microglobulin, host antibodies (IgM, IgG1, and IgG3), and complement components (C1QB and C4B), suggesting platelet opsonization may contribute to thrombocytopenia. Flow cytometry revealed that MHC-I expression in infection is restricted to a subset of platelets (~10%) with elevated forward scatter (Figure 1K, L). Platelets have been previously shown to express MHC-I and be capable of presenting antigen to CD8 T cells [28] but their contribution to T cell activation in schistosomiasis is as yet untested.

Given elevated platelet PS and extensive liver pathology in schistosomiasis, we next assessed the impact of infection on the coagulation cascade. To do this, we developed, a longitudinal coagulometry assay to measure the intrinsic and extrinsic coagulation pathways in mice during infection. This revealed that although PT and aPTT were unchanged during acute infection (8 weeks), both are prolonged during the chronic phase (10–12 weeks) (Figure 2A, B), which is consistent with findings from human schistosomiasis [4,6,7,29]. Together, our data suggest that while platelets appear primed for aggregation in schistosome infection, coagulation is significantly impeded. This contrasts with previous studies by Da'dara et al. (2016) [10] who used thromboelastography (TEG) to show blood from schistosome-infected mice clotted faster than naive animals, but thrombi were rapidly degraded [10]. This discrepancy may reflect differences in time points (7 weeks vs 10–12 weeks), cercarial dose and associated disease pathology (~125 vs 35–50 cercariae), or lack of differentiation between the intrinsic and extrinsic coagulation pathways. Prolonged coagulation may be caused by impeded hepatocyte coagulation factor production due to infection-induced granulomatous inflammation, and/or excessive consumption of coagulation factors [30]. Disseminated intravascular coagulation (DIC) often manifests with prolonged PT and aPTT alongside formation of microthrombi in tissues [31]. We found enhanced $CD41^+$ staining in the liver of schistosome-infected mice that increased with infective dose (Figure 2C). $CD41^+$ clusters represent both microthrombi and multinucleated megakaryocytes, the former distinguished by their absence of nucleus and large size (>150 μm in diameter). These are likely caused by trapped parasite eggs that induce inflammation, sinusoidal damage and rupture. This in turn could promote extensive extrinsic pathway activation and thrombin production, driving a feed-forward loop and coagulation factor consumption [31]. This is consistent with faster coagulation times at earlier time points (i.e., 7 weeks [17]) before severe coagulation factor consumption, and may also contribute to thrombocytopenia as platelets are consumed within microthrombi [10]. There is some evidence for disseminated intravascular coagulation in human schistosomiasis patients [7].

In summary, we have shown that schistosomiasis causes thrombocytopenia, enhanced platelet aggregation and prolonged coagulation. Infection causes large changes to the platelet proteome and future studies are needed to assess the functional drivers of enhanced aggregation. Infection also causes a multifaceted coagulopathy with slower intrinsic and extrinsic coagulation pathways likely reflecting the

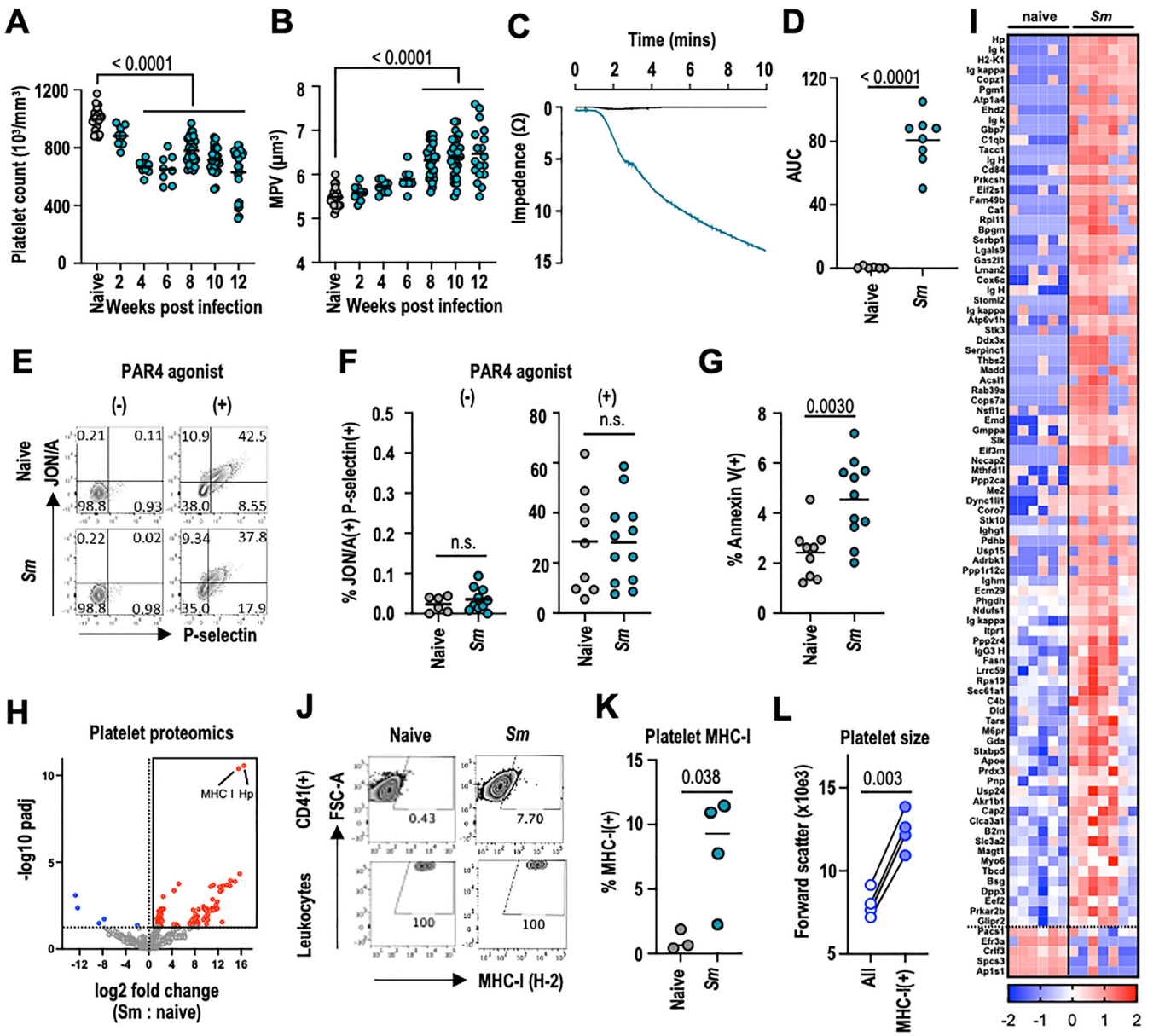

Figure 1 Schistosome infection causes thrombocytopenia, spontaneous platelet aggregation and platelet phenotypic changes. C57BL/6 mice were infected with 35–50 *S. mansoni* cercariae (**A**) platelet counts and (**B**) mean platelet volume (MPV) were determined before and at 2-week intervals after infection. Data is pooled from 2 to 4 experiments with n = 5 per group. (**C**) Whole blood aggregometry in the absence of exogenous stimulation and (**D**) area under the curve (AUC) of impedance (naive n = 6, *Sm* n = 8). (**E**) Representative flow cytometry staining and (**F**) scatter plots for platelet P-selectin and JON/A -/+ PAR4 agonist AYPGKF-NH2. (**G**) Annexin V+ platelets from naïve and 12 week infected mice. Data in F-G pooled from 2 experiments with n = 4–6 per group. (**H**) Volcano plot of platelet proteomics comparing naïve and infected mice. Proteins significantly up/down regulated in infected mice are shown in red and blue, respectively. (**I**) Heat map showing Z-scores for differentially expressed proteins in individual mice (naive n = 6, Sm n = 7). (**J**) Representative flow cytometry staining and (**K**) scatter plots of MHC-I by platelets from blood of naïve and 12 week infected mice (naive n = 3, *Sm* n = 4). Blood leukocyte MHC-I expression included in (**J**) for comparison. (**L**) Paired comparison of forward scatter for all platelets vs. MHC-I(+) platelets in mice at 12 week postinfection. Significance determined by unpaired (**A, B, D, F, G, K**) or paired t test (**L**).

impact of inflammation, impaired coagulation factor production due to liver damage, and/or DIC-induced coagulation factor consumption. The impact of infection-induced changes to hemostasis and coagulation, and their potential reversal following curative anthelminthic praziquantel treatment, should be considered in infected people.

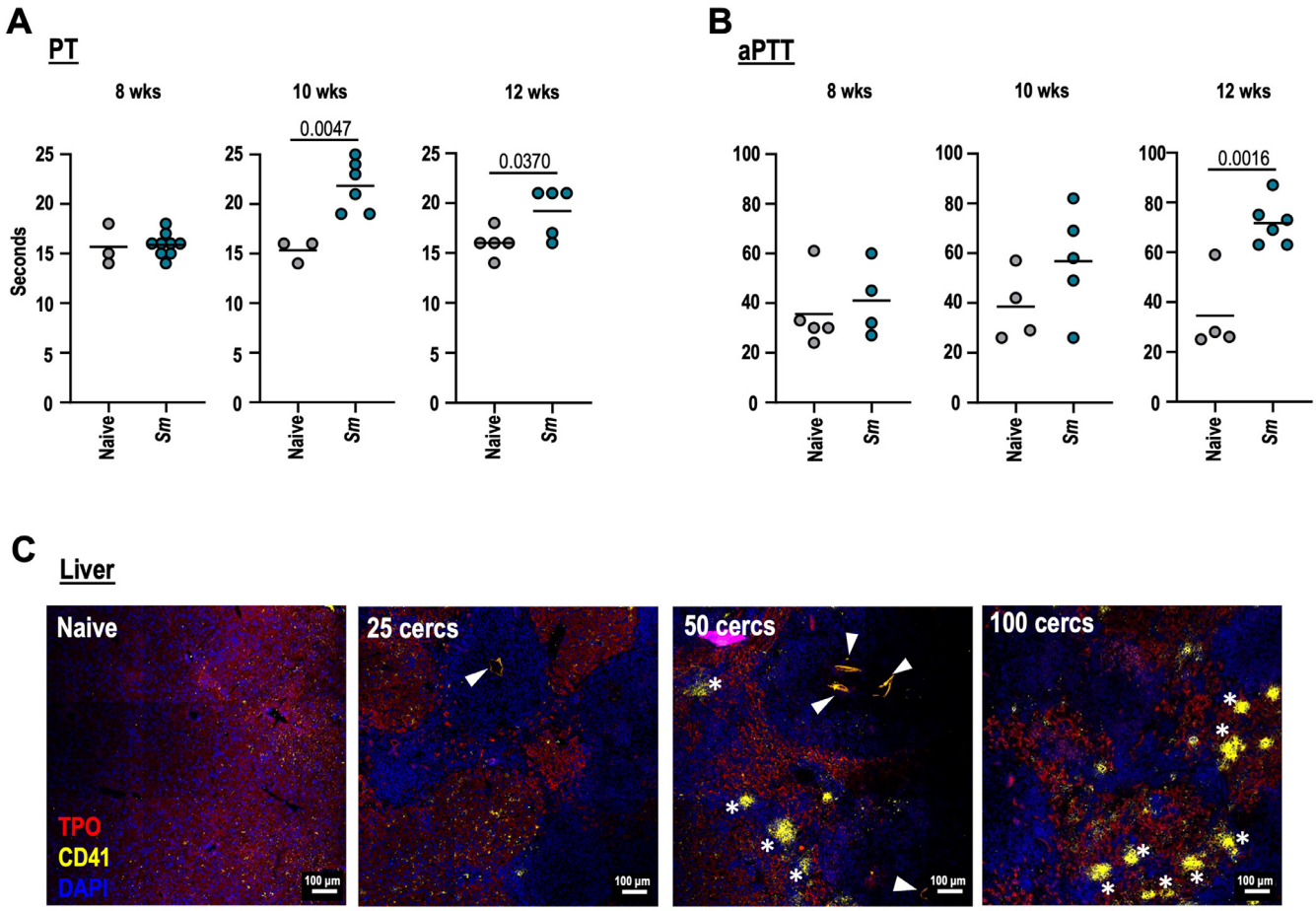

Figure 2 Schistosome infection causes delayed intrinsic and extrinsic coagulation pathways coincident with liver microbleeds. (**A**) Prothrombin time (PT) and (**B**) activated partial thromboplastin time (aPTT) in naive and infected (8, 10 and 12 weeks postinfection) C57BL/6 mice (naive, n = 3–5, *Sm* n = 6–9). Mice were infected with 40 cercariae and significance determined by unpaired t test. (**C**) Representative fluorescent images of liver tissue from naive and infected C57BL/6 mice (infection doses of 25, 50, 100 cercariae) stained for thrombopoietin (TPO, red, hepatocytes), CD41 (yellow, platelets and megakaryocytes) and DAPI (blue). Microthrombi are indicated by asterisks, and autofluorescent schistosome eggs are indicated by arrowheads. Liver samples taken at 12 weeks (25–50 cercariae) or 7 weeks (100 cercariae).

Conflicts of Interest Disclosure

The authors do not have any conflicts of interest to declare in relation to this work.

Acknowledgments

We thank staff in the Biological Services Facility (animal husbandry) and Bioscience Technology Facility Imaging and Cytometry laboratory (flow cytometry and confocal microscopy, University of York). We thank Dr. Benjamin Hulme and Prof. Karl Hoffmann (Aberystwyth University) for providing schistosome-infected snails.

Author Contributions

JHG, JPH, and ISH conceived and designed the research, analyzed, and interpreted the data, and wrote the manuscript. JHG, LM, and SC performed experiments. BJW, JP, and PN carried out and supported the proteomics analysis. All authors read and provided comments on the final manuscript.

Funding

This work was supported by UK BBSRC White Rose Mechanistic Biology Doctoral Training Partnership award to JHG, UK MRC New Investigator Research Grant (MR/W018578/1) and Academy of Medical Science GCRF Springboard (SBF003\1096) to JPH, and Novo Nordisk Foundation (NNF18OC0053231) and Danish Council for Independent Research (DFF-1032-00242B) to BJW and PLN.

SUPPLEMENTARY MATERIALS

Supplementary material associated with this article can be found in the online version at https://doi.org/10.1016/j.exphem.2024.104689.

REFERENCES

1. McManus DP, Dunne DW, Sacko M, Utzinger J, Vennervald BJ, Schistosomiasis Zhou XN. Nat Rev Dis Primers 2018;4:13.
2. Schistosomiasis [Internet]. WHO. [cited 2023 May 1]. Available from: https://www.who.int/news-room/fact-sheets/detail/schistosomiasis.
3. LoVerde PT. Schistosomiasis. Adv Exp Med Biol 2019;1154:45–70.
4. Eyayu T, Zeleke AJ, Seyoum M, Worku L. Basic coagulation profiles and platelet count among Schistosoma mansoni-infected adults attending Sanja Primary Hospital, Northwest Ethiopia. Res Rep Trop Med. 2020;11:27–36.
5. Vasconcellos LS, Petroianu A, Romeiro JR, Tavares Junior WC, Resende V. Correlation between the values of circulating blood elements with the size of spleen in the presence of schistosomal splenomegaly. Acta Cirúrgica Brasileira 2018;33:1103–9.
6. Leite LA, Pimenta Filho AA, Martins da Fonseca CS, et al. Hemostatic dysfunction is increased in patients with hepatosplenic schistosomiasis mansoni and advanced periportal fibrosis. PLoS Negl Trop Dis 2013;7:e2314.
7. Omran SA, el-Bassiouni NE, Hussein NA, Akl MM, Hussein AT, Mohamed AA. Disseminated intravascular coagulation in endemic hepatosplenic schistosomiasis. Haemostasis 1995;25:218–28.
8. Houlder EL, Stam KA, Koopman JPR, et al. Early symptom-associated inflammatory responses shift to type 2 responses in controlled human schistosome infection. Sci Immunol 2024;9:eadl1965.
9. Ngaiza JR, Doenhoff MJ. Blood platelets and schistosome egg excretion. Proc Soc Exp Biol Med 1990;193:73–9.
10. Da'dara AA, de Laforcade AM, Skelly PJ. The impact of schistosomes and schistosomiasis on murine blood coagulation and fibrinolysis as determined by thromboelastography (TEG). J Thromb Thrombolysis 2016;41:671–7.
11. Femoe UM, Jatsa HB, Greigert V, et al. Pathological and immunological evaluation of different regimens of praziquantel treatment in a mouse model of Schistosoma mansoni infection. PLOS Neglected Tropical Diseases 2022;16:e0010382.
12. Schmid AM, Razim A, Wysmołek M, et al. Extracellular vesicles of the probiotic bacteria E. coli O83 activate innate immunity and prevent allergy in mice. Cell Communication and Signaling 2023;21:297.
13. Cox J, Mann M. MaxQuant enables high peptide identification rates, individualized p.p.b.-range mass accuracies and proteome-wide protein quantification. Nat Biotechnol 2008;26:1367–72.
14. Tyanova S, Temu T, Sinitcyn P, et al. The Perseus computational platform for comprehensive analysis of (prote)omics data. Nat Methods 2016;13:731–40.
15. Xie Z, Bailey A, Kuleshov MV, et al. Gene set knowledge discovery with Enrichr. Curr Protoc 2021;1:e90.
16. Amison RT, Cleary SJ, Riffo-Vasquez Y, Bajwa M, Page CP, Pitchford SC. Platelets play a central role in sensitization to allergen. Am J Respir Cell Mol Biol 2018;59:96–103.
17. Bhattacharjee S, Banerjee M. Immune thrombocytopenia secondary to COVID-19: a systematic review. SN Compr Clin Med 2020;2:2048–58.
18. Rani GF, Preham O, Ashwin H, Brown N, Hitchcock IS, Kaye PM. Dissecting pathways to thrombocytopenia in a mouse model of visceral leishmaniasis. Blood Advances 2021;5:1627–37.
19. Handtke S, Thiele T. Large and small platelets—(When) do they differ? Thromb Haemost 2020;18:1256–67.
20. Elzoheiry M, Da'dara AA, deLaforcade AM, El-Beshbishi SN, Skelly PJ. The essential ectoenzyme smnpp5 from the human intravascular parasite Schistosoma mansoni is an ADPase and a potent inhibitor of platelet aggregation. Thromb Haemost 2018;118:979–89.
21. Elzoheiry M, Da'dara AA, Nation CS, El-Beshbishi SN, Skelly PJ. Schistosomes can hydrolyze proinflammatory and prothrombotic polyphosphate (polyP) via tegumental alkaline phosphatase, SmAP. Mol Biochem Parasitol. 2019;232:111190.
22. Bhardwaj R, Skelly PJ. Characterization of schistosome tegumental alkaline phosphatase (SmAP). PLoS Negl Trop Dis 2011;5:e1011.
23. Michelson AD, Furman MI. Laboratory markers of platelet activation and their clinical significance. Curr Opin Hematol 1999;6:342–8.
24. Bergmeier W, Schulte V, Brockhoff G, Bier U, Zirngibl H, Nieswandt B. Flow cytometric detection of activated mouse integrin αIIbβ3 with a novel monoclonal antibody. Cytometry 2002;48:80–6.
25. Naeini MB, Bianconi V, Pirro M, Sahebkar A. The role of phosphatidylserine recognition receptors in multiple biological functions. Cell Mol Biol Lett 2020;25:23.
26. Lentz BR. Exposure of platelet membrane phosphatidylserine regulates blood coagulation. Prog Lipid Res 2003;42:423–38.
27. Reddy EC, Rand ML. Procoagulant phosphatidylserine-exposing platelets in vitro and in vivo. Front Cardiovasc Med 2020;7:15.
28. Zufferey A, Speck ER, Machlus KR, et al. Mature murine megakaryocytes present antigen-MHC class I molecules to T cells and transfer them to platelets. Blood Adv 2017;1:1773–85.
29. Bisetegn H, Feleke DG, Ebrahim H, Tesfaye M, Gedefie A, Erkihun Y. A comparative cross-sectional study of coagulation profiles and platelet parameters of *Schistosoma mansoni*-infected adults at Haik Primary Hospital, Northeast Ethiopia. Interdiscip Perspect Infect Dis 2022 Jun 27;2022:5954536.
30. Peck-Radosavljevic M. Review article: coagulation disorders in chronic liver disease. Aliment Pharmacol Ther 2007;26(Suppl 1):21–8.
31. Papageorgiou C, Jourdi G, Adjambri E, et al. Disseminated intravascular coagulation: an update on pathogenesis, diagnosis, and therapeutic strategies. Clin Appl Thromb Hemost 2018;24:8S–28S.